Spectrum Analysis of An Ablation-Stabilised Arc in Ice

L. J. Cao and A. D. Stokes
School of Electrical Engineering
The University of Sydney
NSW 2006, Australia

Abstract

The spectrum of an ablation-stabilised arc has been recorded using ice as the test material. The intensity of neutral oxygen lines was found to reach the blackbody radiation limit and subsequently the temperature of the vapour layer was determined by the Planck function. The arc diameter, pressure at stagnation point, arc column temperature and vapour temperature were measured by spectroscopic methods. The results are in agreement with a two-zone, isothermal arc model [7].

1 Introduction

The ablation-stabilised arc is very common in expulsion fuses and puffer circuit breakers. The arc is of high current-density being confined in a narrow channel and radiation is the dominant energy-transfer process. Strong radiation causes wall material ablation and a vapour layer exists between the arc column and wall. High pressure is built up and the arc column consists mainly of wall materials [6,7,9].

Under the powerful ablation conditions associated with expulsion fuses, it is normally impossible to view the interior space of the high-current arc. By selecting ice as the confining material, no solid products were produced during arc ablation and it has been possible to record the spectrum of such an arc without the obscuring effect of solid particles.

Among the previous experimental measurements of the arc characteristics [10,11,12], there has been no attempt at spectroscopic temperature measurement. In this paper, the spectrum of the ablation-stabilised arc was taken by side-on spectroscopy and was recorded on a photographic plate. The arc temperature, pressure and diameter were measured by using these results. The test material was a block of ice. The length of the bore was 110 mm and the diameter 10 mm. The theoretical characteristics of such an arc have been calculated in advance [6,11].

2 Preliminaries

2.1 Optical setup

A ray-tracing method [4] was used to calculate the optical setup, in which Gaussian optics is described by matrices. Two doublets were used in this system so that the location of the images and object-to-image ratio could be easily determined. By considering the diameter of the lens and the maximum aperture angle of the spectrograph, a simple program was written to calculate the position of each lens. Figure 1 is the actual optical setup during the experiment.

A shutter was placed at position S to control the exposure. Exposure time was around 2 ms and it was used in all

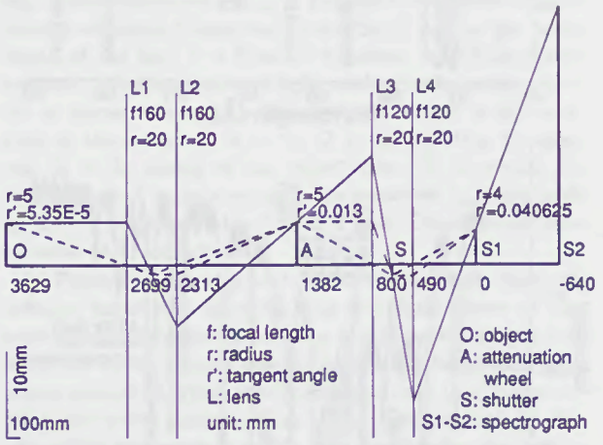

Figure 1: Optical layout of spectrum measurement.

spectral measurements. A Helium-Neon laser beam was used to align the optical elements on the optic axis. A Steinheil universal spectrograph, model GH, and type I-N Kodak photographic plates were used to photograph the arc spectrum. To construct the H-D curve of the plate, an intensity reference spectrum was taken from a standard tungsten filament lamp with an attenuation wheel between the lamp and the spectrograph.

2.2 Influence of the fuse wire

It is well known that metal vapour contamination markedly increases the net radiation emission [13,14], because excitation energy levels of metal atoms are much lower than that of nitrogen and oxygen. The arc column of the ablation-stabilised arc was assumed to be composed of wall-ablation materials.

To investigate the influence of the metal wire on the arc column, two copper wires of different diameters (0.07 mm and 0.35 mm) were used. Spectra were taken from the onset time (0 ms) of the main current to the 9th ms of the first half cycle, in 1 ms steps. The exposure times were around 2 ms. A photomultiplier was mounted inside the spectrograph and its voltage signal was sent to an oscilloscope so that precise exposure time could be recorded.

For a given wire, $\int [i \sin(\omega t)]^2 \, dt$ is a constant. Experimental results showed that it took 0.32 ms to evaporate a 0.07-mm wire at 2.4 kA. Copper lines were observed in the spectra for observation times up to 3-5 ms from onset of the main current. No copper lines were observed for 4-6 ms observation times. Figure 2 shows the spectra of a 2.4-kA arc taken between 2.0-3.9 ms and 4.9-6.8 ms. Strong copper lines can be clearly distinguished for the early exposure (top), while there are no copper lines in the later exposure (bottom).

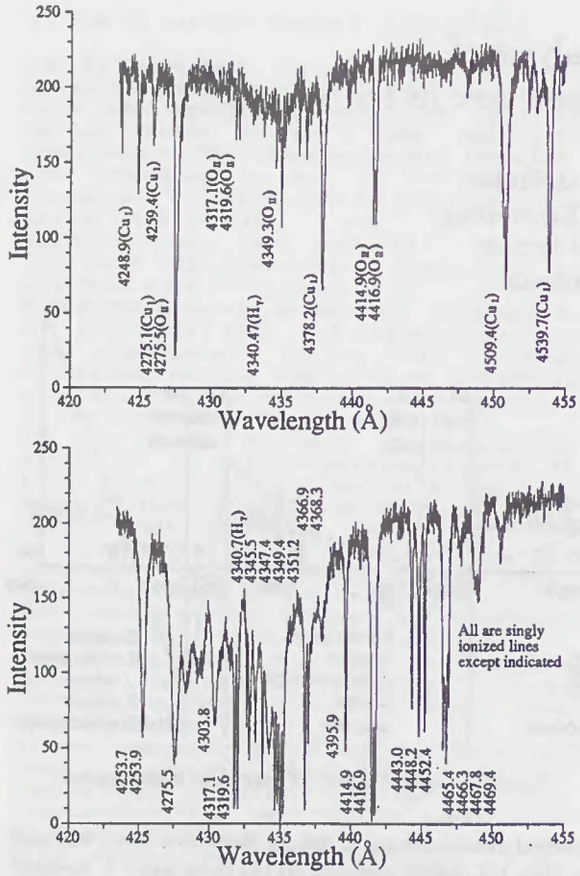

Figure 2: Spectra at 2.0 ms (top) and 4.9 ms (bottom), 0.07-mm wire, 2.4 kA.

By contrast, it took 1.78 ms to evaporate a 0.35-mm wire for a current of 2.4 kA, and copper lines were detected on the plate throughout the first half cycle. Since 0.07-mm fuse wire was used for all experiments, it was not necessary to consider the effect of metal vapour on arc behaviour.

2.3 Spectral line reconstruction

The photographic plate containing the image of the spectral lines was scanned by a microdensitometer. A spectral line reconstruction code [5] was modified to meet the present requirements. The program calculated the H-D curve from scanned data and converted the emulsion density to exposure according to the H-D curve. Then FFT filtering was performed to eliminate noise due to plate granularity, line rotating and bending techniques were used to eliminate the astigmatic effect and Abel inversion was performed to recover the emissivity of the arc cross-section. The maximum exposure was kept below the upper limit of the linear region of the H-D curve.

Figure 3 shows a typical spectral line recovery process on the O II line at 466.1 nm. From top to bottom, there are three-dimensional and contour plots of the emulsion density of the photographic plate, radiance after correction and recovered spectral emissivity, respectively. For the three-dimensional plots, the X axis is in the wavelength direction and the Y axis is in the radial (arc diameter) direction. The axis notation for contour plots is the opposite.

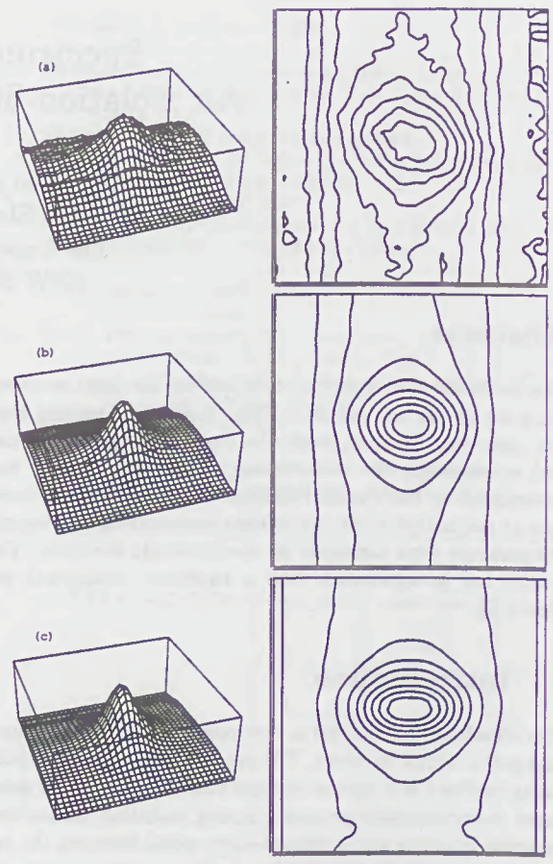

Figure 3: Typical process of spectrum line reconstruction on the singly ionised oxygen line 466.1 nm. See text.

3 Electron density and pressure measurement

If inelastic collisions can be ignored, line broadening by charged particles is mainly attributed to the linear Stark effect in the case of hydrogen. The half-width of the line depends on the electron and ion densities and may be used to measure N_e [15].

The effect of Doppler broadening is much smaller than that of Stark broadening in such a high-pressure arc. The half-width contributed by Doppler broadening is

$$\delta\nu_D = 7.16 \times 10^{-7}\nu_0(T/M)^{1/2},$$

where M is the mass number. At 20 000 K the half-widths of H_α and H_β are 0.66 Å and 0.49 Å, respectively, while they are over 100 Å in this experiment. The effect of Doppler broadening was thus ignored.

For quasi-static (ionic) broadening, the line width is proportional to $N_e^{2/3}$ [1]. The hydrogen lines are well described by the quasi-static model in which the smearing effect from electron impacts changes the line profile but has little effect on the actual half-value width. N_e can be obtained from the relation

$$N_e = C(N_e, \lambda)(\Delta\lambda)^{3/2},$$

where C depends only weakly on N_e and T and it can be found from tables [1,3]. Figure 4 shows the measured half-width and electron number density calculated by equation (3). Fig-

ure 5 shows the calculated pressure [11] and evaluated pressure from measured electron number density. Since, in the LTE condition, the material functions are uniquely determined by temperature and pressure, the pressure was evaluated from the calculated material function table by assuming a theoretical temperature.

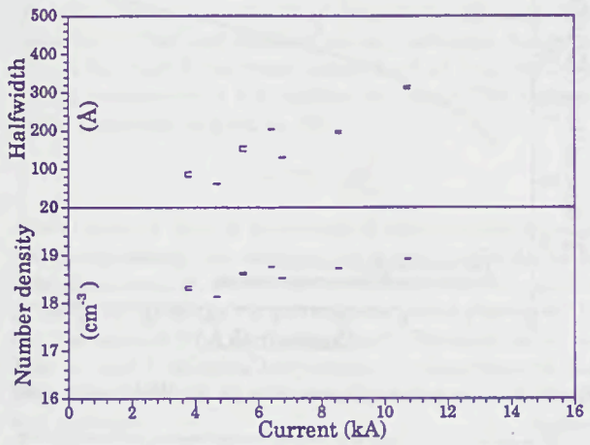

Figure 4: Measured half-width and electron number density.

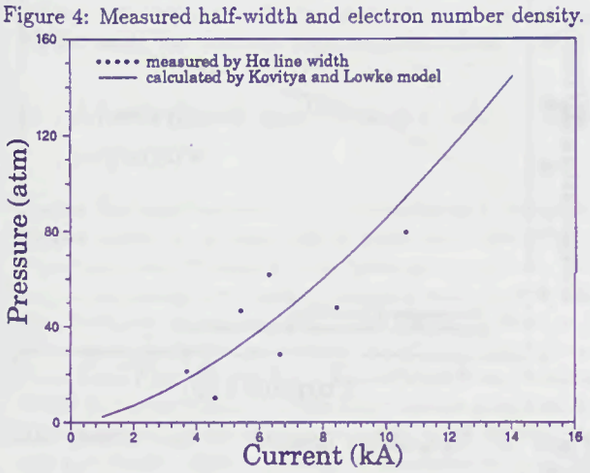

Figure 5: Calculated and measured pressures.

The half-width of the H_α line was widely broadened since the pressure inside the tube was very high. The half-widths of the H_β and H_γ lines were so wide that these lines interfered with each other and therefore could not be used for measurement.

4 Temperature measurement

The transitions of internal energy levels of atoms and ions can be classified into three groups, that is, bound-bound, bound-free and free-free transitions. Bound-bound transitions occur at a particular spectral wavelength and produces a line spectrum of the atomic species. The other two kinds of transition produce a radiation continuum.

Spectroscopic analysis includes measurement of the spectral radiance and identification of the atomic and molecular processes giving rise to the observed spectra. The temperature determination may depend on measurements at a single spectral frequency or on some relationship among measurements at several frequencies.

4.1 Absolute line intensity

Gas temperature can be determined by measuring radiance integrated over the frequency bandwidth of a single line. When self-absorption is negligible, the integrated radiance (I_{nm} in W m^{-3} ster^{-1}) of an atomic emission line is [16,17]

$$I_{nm} = \frac{hc}{4\pi}\rho_0 \frac{g_n}{Q}\frac{A_{nm}}{\lambda_{nm}} e^{-E_n/kT},$$

where the subscripts n and m refer to the upper and lower energy states respectively, A_{nm} is Einstein's coefficient of spontaneous emission (transition probability), λ_{nm} is the wavelength of the line, h is Planck's constant, k is Boltzmann's constant, c is the velocity of light, and ρ_0 is the number density of atoms or ions, g_n is the statistical weight of the upper state of the transition $n \rightarrow m$, Q is the partition function, and E_n is the energy of the upper state. To determine the temperature of a gas specimen, one measures I_{nm}, and looks up the temperature on the I_{nm} *vs.* T plot. One does not solve equation (4.1) explicitly.

Figure 6 shows a typical measurement result. Since the radiance varies with approximately the fourth power of temperature, the decrease of radiance is much greater than that of temperature. Beyond the arc boundary, the measured radiance reduces to a very small value and even to a "negative" value, due to the granular noise of the photograph plate. The edge of the temperature profile then was simply taken as the abrupt of intensity. It can also be seen that the temperature profile is not flat but is higher in the centre.

Figure 7 plots both the measured temperature by the absolute line intensity method and the calculated temperature [11]. Since the temperature profile over radius was not a constant, the experimental points were plotted as a range rather than a point. The upper boundary is the temperature at the arc centre and the lower boundary is the temperature taken at one third of the radius from the arc centre since the variation of radiance and temperature at the edge of the arc column are quite large and can lead to a certain degree of uncertainty there.

4.2 Boltzmann plot and line intensity ratio

Temperature can also be determined from the relative intensities of spectral lines of the same atomic species. When the lines belong to the same ionisation level, the partition functions and number densities of particles in the ground state are the same.

Equation (4.1) can conveniently be re-written [8] to perform the Boltzmann plot,

$$\log \frac{I_{nm}\lambda_{nm}}{g_n A_{nm}} = const - \frac{E_n}{kT}.$$

A plot of $\log I\lambda/gA$ against E for several spectral lines of the same ionisation level should be a straight line of slope $1/kT$. Deviations from the Boltzmann distribution should show up as deviations from the straight line, due to optical depth (absorption). Figure 8 shows such a plot of a 2.4-kA arc.

To compare the intensities of two lines by using equation (4.1), we obtain the equation for the line intensity ratio method [8],

$$\frac{I_1}{I_2} = \frac{A_1 g_1 \lambda_2}{A_2 g_2 \lambda_1} e^{-\frac{E_1 - E_2}{kT}},$$

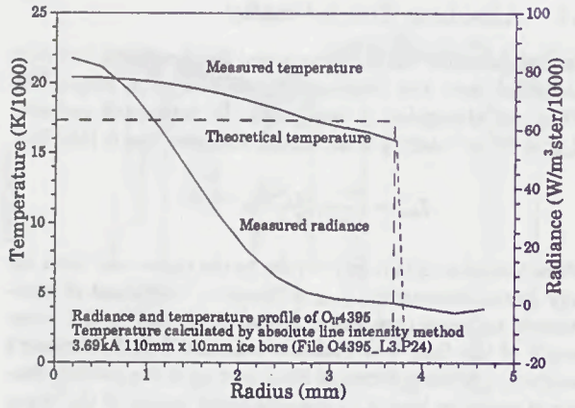

Figure 6: Radiance and temperature profile over arc radius.

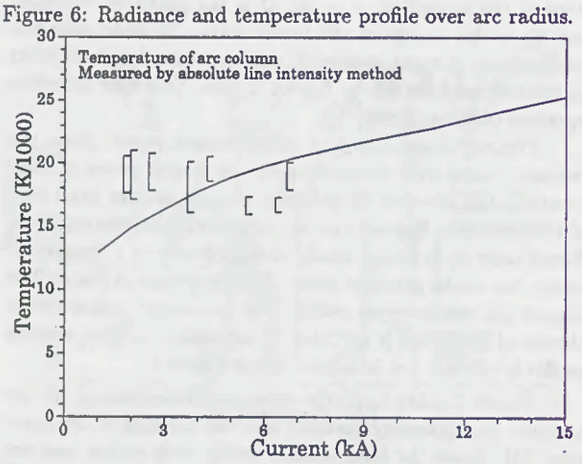

Figure 7: Temperature measured by absolute line intensity method.

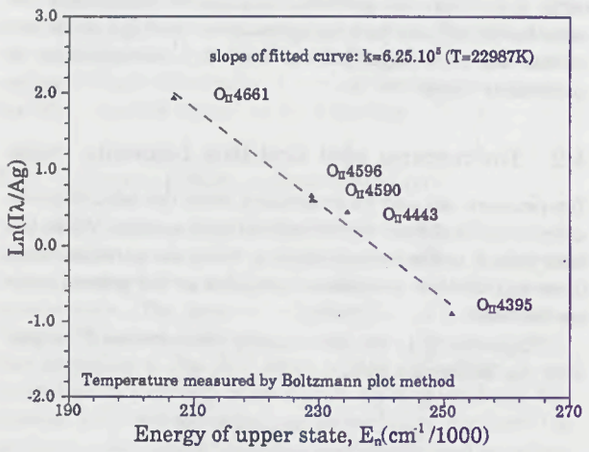

Figure 8: Boltzmann plot.

where the indices 1 and 2 refer to the first and the second line respectively. To be able to evaluate the temperature accurately, the energy difference of the upper terms of the two lines, $E_1 - E_2$, must be large ($\geq 2\,\mathrm{eV}$).

The line intensity ratio method and Boltzmann plot method offer the possibility to evaluate the temperature without knowledge of the number densities and partition functions of the atomic species, which will hopefully bring down the calculation errors. These two methods are basically the same. Figures 9 and 10 are the results of the measurements. The measured temperatures are higher than those calculated, which indicates significant self-absorption.

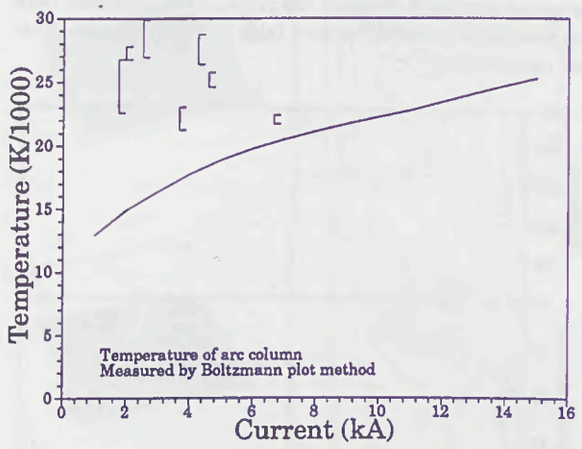

Figure 9: Temperature measurement by Boltzmann plot method.

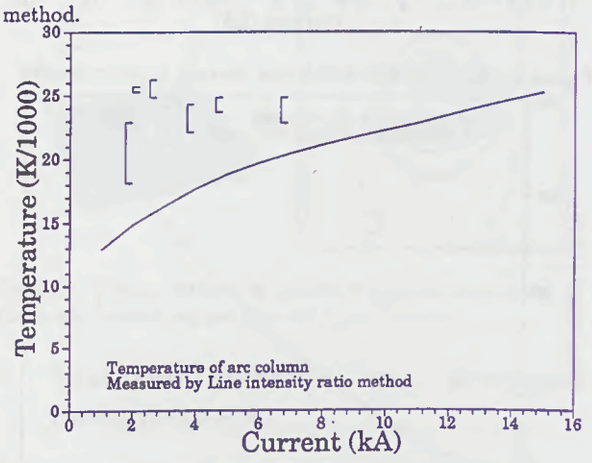

Figure 10: Temperature measured by line intensity ratio method.

4.3 Relative line intensity

As in equation (4.1), the radiance of a single line increases with increase of plasma temperature and number density of the atomic species. At a constant pressure, increase of plasma temperature is accompanied by decrease of number density. As temperature goes higher, the influence of the decrease of number density on the radiance will eventually surpass the influence of the increase of temperature. The radiance will then start to fall off. If a line radiance profile has an off-axis peak, its temperature can be determined by considering the relative intensity of the atomic line, the Fowler-Milne method [2].

One then normalises the maximum of the I *vs.* T plot with the maximum of the I *vs.* r plot. The temperature profile can be determined by matching the maxima of both radiance plots. In the current experiment, neutral oxygen and hydrogen lines were found to have off-centre peaks. It was further found that the measured radiance was 50-100 times lower than expected. With such heavy absorption, the Abel inversion and line intensity methods were no longer applicable. These lines were dealt with differently, as described in

section 5.

4.4 Absolute continuum intensity

Continuum radiation arises from the interaction of initially free electrons with the positive ions or atoms that are present. The interactions may be either free-free transitions (Bremsstrahlung) or free-bound transitions (recombination radiation). The total intensity at any particular frequency $I(\nu)$ is the sum of the contributions from all such processes having components at the specified frequency. The radiance of the continuum is given as [15]

$$I(\nu) = C(\nu)\frac{N_e N_i}{T^{1/2}},$$

where constant $C(\nu)$ is a function of wavelength but not of population density nor temperature in the wavelength range considered here. N_e and N_i are the electron and ion densities respectively. From the known temperature distribution of the arc, the value of $C(\nu)$ can be calculated. The same value can then be used to calculate temperature at other pressures and population densities since it is independent of temperature and pressure.

During the analysis, it was found that $C(\nu)$ was not a constant. It decreases with the increase of current. Again this indicated that self-absorption has taken place.

5 Absorption and vapour layer temperature

The arc has been described by a two-dimensional, isothermal channel model [7]. At large optical depth, each photon must be absorbed and re-emitted many times on its way out. The surface brightness must reach a saturation value equal to that of a blackbody at some points. Thus the major fraction of the energy is dissipated by radiation, which is absorbed in the cooler outer regions of the arc. This self-absorption produces a shelf in the temperature profile as a function of radius. As a consequence, a zone of vapour usually exists between the wall and the arc plasma. Not all of the radiation from the centre of the arc is of a wavelength short enough to ionise the ablated material from the wall. The vapour is transparent to some of the radiation.

As in section 4.3, the intensities of neutral lines was much lower than those of theoretical predictions. A typical radiance profile (O I 715.6 nm) is shown in Figure 11. It can be clearly observed that line profile is flat over a large distance from the axis, which can be explained by Figure 12. At the particular wavelength, the blackbody radiation limit is reached and radiation from the arc core is absorbed almost completely. The line profile recorded on the plate is the intensity profile of the vapour layer. It reaches the saturation value of blackbody radiation. The flat profile is evidence of extremely heavy absorption of the arc radiation.

As the pressure inside the bore becomes large, the radiation intensity approaches the blackbody radiation limit. The line shape will saturate by redistributing its energy within a larger bandwidth. The half-width of singly ionised oxygen lines in this experiment is around 3 Å while that of neutral lines is around 12 Å. Widely spread line-width is further evidence that the blackbody radiation limit has been attained.

On the other hand, larger amounts of particles are concentrated at the related energy levels (centre frequency).

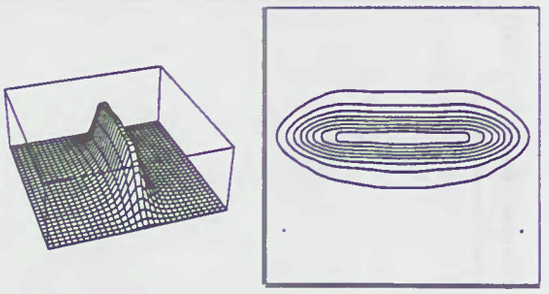

Figure 11: Typical radiance profile of the neutral oxygen line 715.6 nm, continuum extracted).

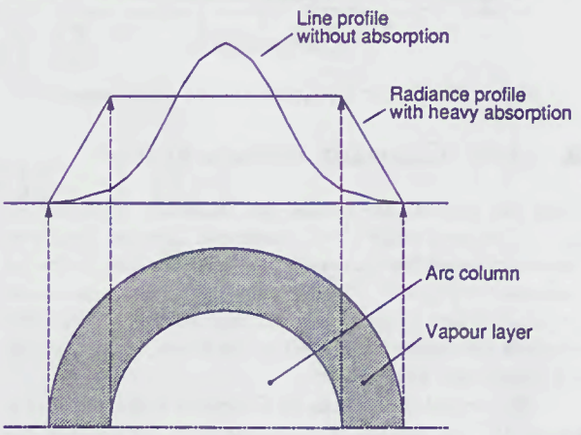

Figure 12: Radiation profile with and without heavy absorption.

This, in turn, will lead to heavy absorption at the line centre. It was observed that both the H_α and H_β lines recorded had a dip at the line centre. This is contrary to the predicted Stark profile for H_α because there are no shifted central Stark components in H_α as there are in H_β. This provides more evidence that heavy absorption is present in the neutral atomic lines. The dip is caused by absorption from particles of very high population density at the centre frequency.

Equation (4.1) was also integrated to evaluate theoretically the extent of line radiation. It was found that the integrated intensity of neutral line radiance approached the blackbody radiation limit under the high pressures in this experiment (same order of magnitude), while that of a singly ionised oxygen lines was far less than the limit (two orders of magnitude lower).

It was thus assumed that the radiation of neutral lines attained the blackbody radiation limit. The distribution of blackbody radiation is governed by the Planck function [15],

$$I_0(\nu, T) = \frac{2h\nu^3}{c^2}\frac{1}{e^{h\nu/kT} - 1}.$$

Thus the vapour layer temperature can be determined from the radiance profile of a neutral line. Figure 13 shows the vapour temperature calculated by this method. We can see that the vapour temperature is almost independent of current. It should be related to a temperature high enough to evaporate all possible solid materials.

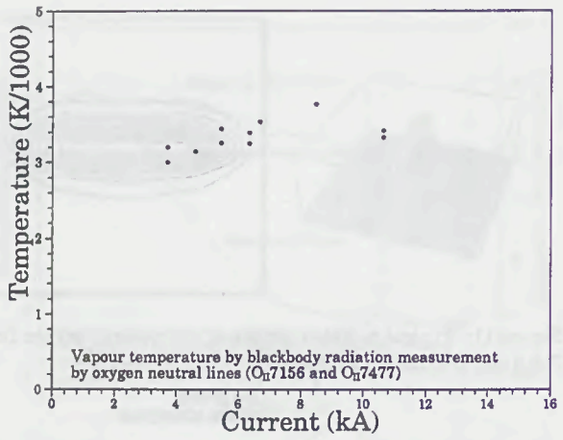

Figure 13: Vapour layer temperature measurement.

6 Arc diameter measurement

Since the spectral line profile was faithfully reconstructed, the arc diameter could also be measured. Two methods were used to measure the diameter of the arc. The first method is illustrated in Figure 6. The arc temperature profile calculated by absolute line intensity method falls abruptly. The point at which this occurs is regarded as the boundary between the arc column and vapour layer.

The second method can be illustrated with references to Figure 11. The flat top of the radiance profile indicates the arc column. The position of the edge is taken as the midpoint between the "shoulder" and "toe". Figure 14 shows the results of diameter measurement by these two methods. The measurement fits well with the theoretical prediction.

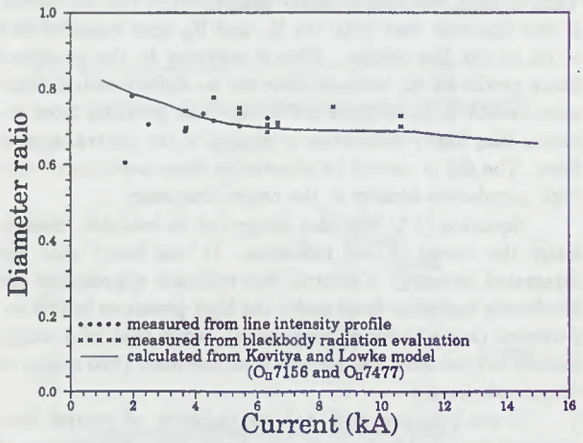

Figure 14: Diameter measurement.

7 Discussion

Because of the presence of self-absorption, temperature calculation through intensity measurements in Section 4 is not very accurate. As the current density and pressure increase, spectral transmissivity decreases. Thus, temperature measured by absolute line intensity of singly ionised oxygen lines is lower at higher current (Figure 7). Absorption leads to a higher population of atoms at lower excitation energy levels. As a result, the measured intensities at lower energy level are lower than they should be, because radiation at these levels is more likely to be absorbed. Because of this reason, the points on the left side of Figure 8 are lower than they should be. Subsequently, the slope is too low and temperatures on Figure 9 and 10 are too high.

The Stark broadening mechanism is independent of the state of LTE. The pressure evaluation in section 3 is fairly accurate, by using measured electron number density and theoretical temperature. This in turn indicates that the temperature predicted is correct.

Comparing Figures 3(b) with Figure 11, we can see that the radiance of the neutral oxygen line is spread through the outer layer while the radiance of the singly ionised oxygen line is concentrate at the centre. This is because there are two zones in the channel, a high temperature arc column and a low temperature vapour layer. It also explains why lines of different energy level are present on the same photographic plate.

Acknowledgment

The authors wish to thank Prof. T. Lipski and Dr. A. J. D. Farmer for helpful advice.

References

[1] J Cooper. *Reports on progress in physics*, Vol.29(Part 1):35–130, 1966.

[2] R H Fowler and E A Milne. *Monthly Notices Roy. Astron. Soc. (London)*, Vol.83, 1923.

[3] H R Griem. *Plasma spectroscopy*, McGraw-Hill Book Company, 1964.

[4] K Halbach. *Am. J. Phys.*, Vol.32:90–108, 1964.

[5] C A Schmidt-Harms. Internal Report, School of Elec. Eng., Univ of Sydney. 1985.

[6] P Kovitya. *IEEE Tran. on Plasma Science*, Vol.15:294–301, 1987.

[7] P Kovitya and J J Lowke. *J. Phys. D: Appl. Phys.*, Vol.17:1197–1212, 1984.

[8] W Lochte-Holtgreven. *Plasma diagnostics*, North-Holland Publishing Company. 1968.

[9] L Niemeyer. *IEEE Tran on PAS*, Vol.97:950–958, 1978.

[10] C B Ruchti and L Niemeyer. *IEEE Trans on Plasma Science*, Vol.14:423–434, August 1986.

[11] A D Stokes and L J Cao *J. Phys. D: Appl. Phys.*, Vol.22:1697–1701, 1989

[12] A D Stokes, H Sibilski and P Kovitya. *J. Phys. D: Appl. Phys.*, Vol.22:1702–1707, 1989

[13] D C Strachan. *Proc. IEE*, Vol.123(11), 1976.

[14] D C Strachan. *J. Phys. D: Appl. Phys.*, Vol.10:361–370, 1977.

[15] A P Thorne, *Spectrophysics*, Chapman and Hall & Science Paperbacks. 1972.

[16] R H Tourin, *Spectroscopic gas temperature measurement*, Elsevier Publishing Company, 1966.

[17] W L Wiese, M W Smith and B M Glennon, *Atomic transition probabilities*, Vol.1, NBS 4, 1966; Vol.2, NBS 22, 1969.

Session 2

FUSE DESIGN II